Published online December 15, 2004

Nucleic Acids Research, 2004, Vol. 32, No. 22 ***e184***
doi:10.1093/nar/gnh182

Tris-borate is a poor counterion for RNA: a cautionary tale for RNA folding studies

Karen L. Buchmueller and Kevin M. Weeks*

Department of Chemistry, University of North Carolina, Chapel Hill, NC 27599-3290, USA

Received August 31, 2004; Revised November 19, 2004; Accepted November 29, 2004

ABSTRACT

Native polyacrylamide gel electrophoresis is a powerful approach for visualizing RNA folding states and folding intermediates. Tris-borate has a high-buffering capacity and is therefore widely used in electrophoresis-based investigations of RNA structure and folding. However, the effectiveness of Tris-borate as a counterion for RNA has not been systematically investigated. In a recirculated Hepes/KCl buffer, the catalytic core of the bI5 group I intron RNA undergoes a conformational collapse characterized by a bulk transition midpoint, or $Mg_{1/2}$, of ~3 mM, consistent with extensive independent biochemical experiments. In contrast, in Tris-borate, RNA collapse has a much smaller apparent $Mg_{1/2}$, equal to 0.1 mM, because in this buffer the RNA undergoes a different, large amplitude, folding transition at low Mg^{2+} concentrations. Analysis of structural neighbors using a short-lived, RNA-tethered, photocrosslinker indicates that the global RNA structure eventually converges in the two buffer systems, as the divalent ion concentration approaches ~1 mM Mg^{2+}. The weak capacity of Tris-borate to stabilize RNA folding may reflect relatively unfavorable interactions between the bulky Tris-borate ion and RNA or partial coordination of RNA functional groups by borate. Under some conditions, Tris-borate is a poor counterion for RNA and its use merits careful evaluation in RNA folding studies.

INTRODUCTION

A detailed understanding of the principles that govern RNA folding remains an important, incompletely understood problem in biology. A fundamental observation is that the architecture of both simple and multi-helix structures and of large complexly folded RNAs is strongly dependent on the Mg^{2+} concentration. One powerful approach for understanding RNA folding reactions has, therefore, been to visualize the mobility of an RNA using 'native' polyacrylamide gel electrophoresis as a function of Mg^{2+} concentration. Native gel approaches have been productively employed to evaluate the folding of the hammerhead ribozyme (1), the hairpin ribozyme (2,3), tRNA (4), viral RNAs, the Tetrahymena group I intron and its domains (5–8), and the catalytic core of the bI5 group I intron (9). In many cases, conclusions drawn from native gel electrophoresis experiments have been corroborated using complementary physical methods (2,7–11).

Gel electrophoresis has many advantages for monitoring RNA folding reactions. The technology is simple and inexpensive, allows structural characterization of multiple RNAs or RNA mutants in a single experiment, and facilitates the detection of alternate conformers and folding intermediates as species with distinct electrophoretic mobilities. The buffer most widely used in gel electrophoresis experiments is Tris-borate (pH ~8.5). The Tris and borate ions form a chair-like six membered ring chelate zwitterion (Figure 1) (12). The aqueous Tris-borate chelate has near-neutral charge overall (12,13), migrates slowly under electrophoresis, and thus has an advantageous high-buffering capacity. Because Tris-borate is such a useful electrophoresis buffer, investigators have, in some cases, chosen to perform non-electrophoresis-based experiments in Tris-borate in order to be able to compare the latter experiments with a Tris-borate 'standard state'.

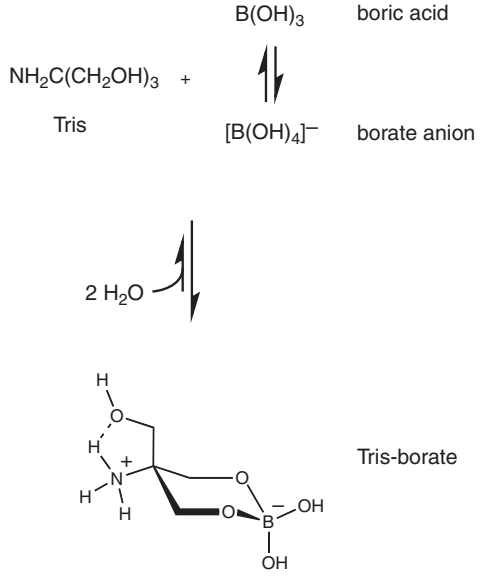

Figure 1. Formation and structure of Tris-borate (12,13).

*To whom correspondence should be addressed. Email: weeks@unc.edu

Ideally, the buffer should not interact significantly with the system under study. However, there is a significant precedent that the buffer is not always a passive spectator for reactions involving nucleic acids. Buffer choice has been shown to have a significant effect on nucleic acid–protein (14), nucleic acid–small molecule (15) and nucleic acid hybridization (16) reactions. In addition, borate ions can form direct ligand complexes with the functional groups present in nucleic acids (17,18).

In exploratory work designed to monitor conformational collapse of the catalytic core of the bI5 group I intron RNA, we noticed that the Mg^{2+} dependence for conformational collapse was dramatically different depending on whether gel electrophoresis experiments were performed in Hepes/KCl or in Tris-borate buffers. Following up on this observation, we found that the catalytic core of the bI5 RNA is less structured at low magnesium ion concentrations in Tris-borate than in Hepes/KCl. In the Hepes/KCl buffer system, folding of the bI5 RNA is well characterized as proceeding from expanded, to near-native collapsed, to native states as the $MgCl_2$ concentration is increased from 0 to 40 mM (9,11,19,20). Similar states appear to form in Tris-borate with the significant difference that the denaturing character of Tris-borate causes the RNA to form an even-more-expanded state at low Mg^{2+} concentrations.

MATERIALS AND METHODS

Solution and native gel conditions

Folding experiments were carried out in either Hepes/KCl [50 mM Hepes (pH 7.6) and 50 mM KCl] or Tris-borate [90 mM Tris-borate (pH 8.5) and 0.1 mM EDTA] plus $MgCl_2$. Electrophoresis was performed at 35°C using 6% (29:1; acrylamide/bisacrylamide) gels with a thermostatted apparatus and efficient buffer recirculation using a peristaltic pump. RNAs were heated to 90°C and placed on ice prior to loading on the gel. Experiments in Hepes/KCl were performed with radiolabeled RNA; gel origins were labeled by brief electrophoresis of additional radiolabeled RNA prior to disassembling the gel (9). Tris-borate experiments were visualized by ethidium bromide staining. To facilitate visual comparison with the Hepes/KCl data, black and white images of scanned Tris-borate gels were reversed using image analysis software. All RNAs were initially refolded in 50 mM Hepes, 50 mM KCl and $MgCl_2$; once subjected to electrophoresis, ion concentrations reflect those of the gel and the recirculated running buffer.

Photocrosslinking

The 5′-^{32}P-end labeled bI5core RNA with a single, site-specific, photoactivatable arylazide at position U84 was created via a continuous semi-synthesis (11). Crosslinker-derivatized RNA was denatured by heating to 90°C and then quickly cooled on ice prior to the addition of either Hepes/KCl (supplemented with 0.1 mM EDTA) or Tris-borate buffer, and $MgCl_2$. Cross-linking was induced by incubation of the RNA over a 300 nm, polystyrene filtered ultraviolet (UV) light source for 10 min (21). Cross-linking was quenched by the addition of DTT to 90 mM final concentration and the cross-linked products were visualized on denaturing 8% polyacrylamide gels (11).

RESULTS AND DISCUSSION

The catalytic core of the bI5 group I intron as a model for folding of large RNAs

We compared the effect of buffer choice on RNA structure using the catalytic core of the bI5 group I intron (termed bI5core RNA) as a model system (Figure 2A). The bI5core RNA is a good model for the widespread class of RNAs that require protein co-factors to assume their functional state under physiological ion conditions. The structure of this RNA varies as a function of the magnesium ion concentration. In a Hepes/KCl buffer system [50 mM Hepes (pH 7.6) and

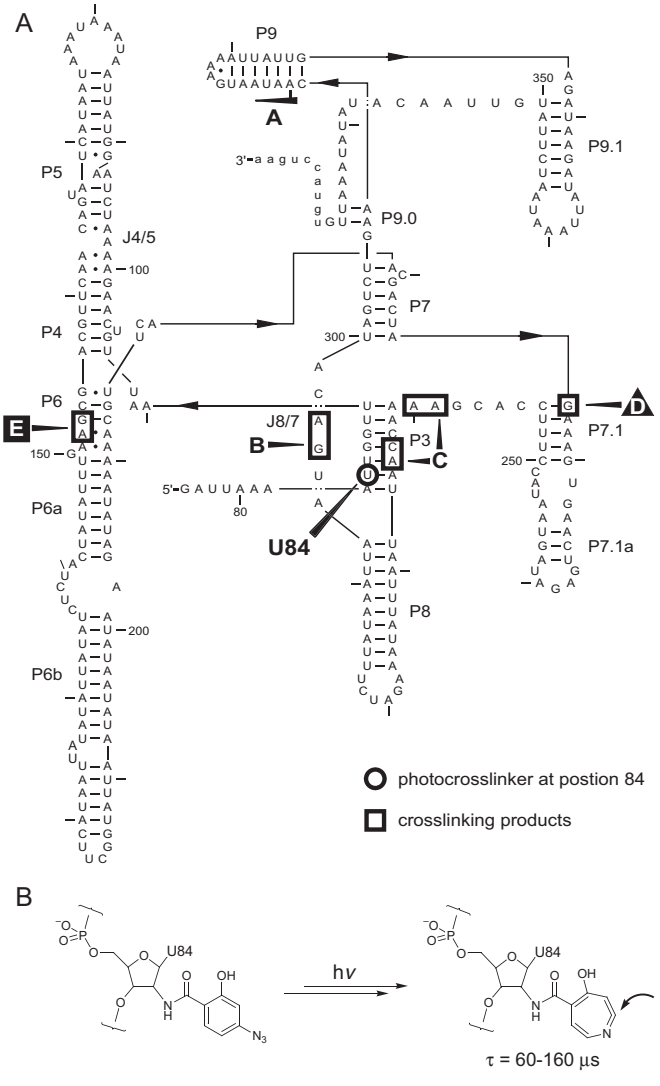

Figure 2. Structure of the bI5core RNA and cross-linking partners with position U84. (**A**) Cross-links A, B and C report native interactions. Cross-link D (white letter on black triangle) reports a transient interaction and cross-link E (white letter on black box) reports an expanded state interaction. Cross-linking partners (B–E) were mapped to nucleotide resolution by primer extension (11); cross-link A lies 3′ of position 310. (**B**) RNA-tethered photocrosslinking via a short-lived ketenimine electrophile (21).

50 mM KCl], but in the absence of Mg^{2+}, the bI5core RNA exists in an expanded state (9) characterized by stable formation of terminal stem–loop structures and a relatively fluid core (22). At 7 mM Mg^{2+}, the bI5core RNA forms a near-native collapsed state whose overall structure lies very near to that of the native state (11,20). The bI5core RNA folds to the native state either upon binding by its CBP2 protein cofactor or in the presence of 20–40 mM Mg^{2+} (19,23).

Large differences in RNA collapse profiles measured in Hepes/KCl versus Tris-borate buffers

The global structure of the bI5core RNA was initially monitored using native gel electrophoresis in the Hepes/KCl buffer, using a thermostatted electrophoresis chamber and efficient buffer recirculation (9). RNA mobilities were compared with two kinds of markers: a double-stranded DNA (dsDNA) ladder in 100 bp increments and a 186 bp dsRNA. Consistent with prior work (9), the mobility of the bI5core RNA is similar to that of the 300 bp DNA marker in the absence of Mg^{2+} (compare marker, M, and bI5core lanes in left most panel in Figure 3A). When native gel experiments are performed at increasing Mg^{2+} concentrations, the mobility of the bI5core RNA increases relative to that of the DNA and RNA markers, until plateauing by ~20 mM $MgCl_2$ (Figure 3A). The measured mobility of the bI5core RNA was normalized to that of the dsRNA marker and plotted as a function of Mg^{2+} concentration; the

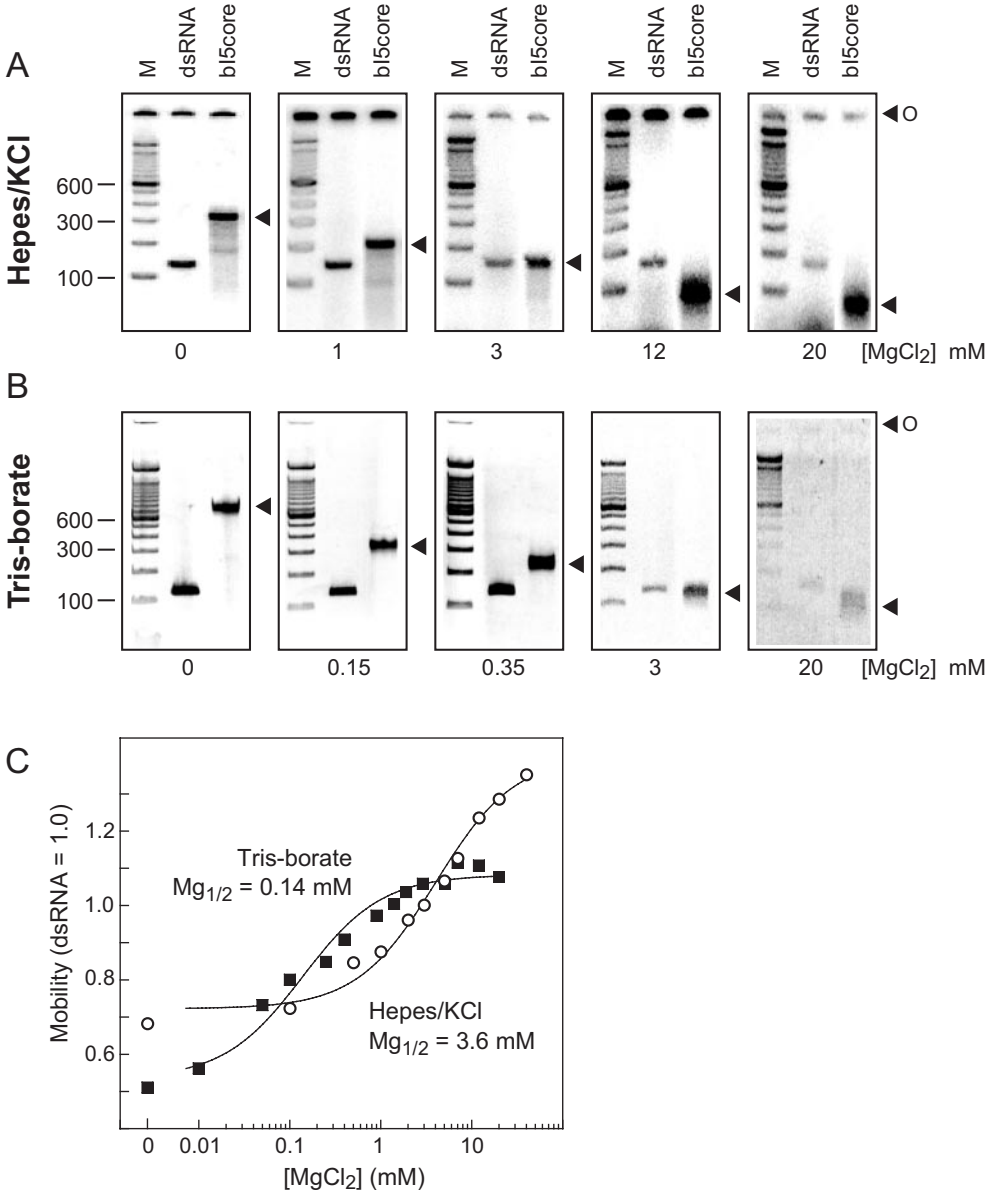

Figure 3. Collapse of the bI5core RNA visualized using native gel electrophoresis. Electrophoresis was performed in Hepes/KCl (**A**) or Tris-borate (**B**) buffers. In order to show each collapse transition clearly, different $MgCl_2$ concentrations are shown in (A and B). Markers are a 100 bp DNA ladder (M) or a 174 bp dsRNA. Triangles to the right of each gel indicate the mobility of the bI5core RNA; O is the gel origin. (**C**) Electrophoretic mobility of the bI5core RNA in Hepes/KCl (open circles) and Tris-borate (closed squares), normalized to that of the dsRNA marker. Relative mobility = $A\{[Mg^{2+}]/(Mg_{1/2} + [Mg^{2+}])\} + Mg_0$, where A is the transition amplitude, $Mg_{1/2}$ is the transition midpoint and Mg_0 is the mobility observed in the absence of $MgCl_2$.

transition midpoint ($Mg_{1/2}$) is 3.6 mM (open circles in Figure 3C).

A similar series of experiments were performed as a function of $MgCl_2$ concentration, but using 90 mM Tris-borate as the electrophoresis buffer. In this buffer system, the dsDNA and RNA markers maintain the same mobility relative to each other as observed in the Hepes/KCl buffer system (compare DNA marker, M, and dsRNA lanes in Figure 3A and B). In the absence of magnesium ion, mobility of the bI5core RNA is significantly reduced in Tris-borate relative to that observed in Hepes/KCl buffer; the bI5core RNA mobility is similar to that of the 800 bp dsDNA in Tris-borate (left-hand panel in Figure 3B). At 3 mM $MgCl_2$, the ion-dependent folding profiles converge such that the mobility of the bI5core RNA is similar to that of the dsRNA marker in both Tris-borate and Hepes/KCl (see 3 mM panels in Figure 3A and B). The mobility of the bI5core RNA increases with increasing Mg^{2+} concentrations in Tris-borate and, again, plateaus by 20 mM $MgCl_2$. However, when the normalized mobility is plotted as a function of Mg^{2+} concentration, the apparent $Mg_{1/2}$ is 0.14 mM (closed squares in Figure 3C), which is much lower than the folding transition measured in Hepes/KCl.

Thus, relative to the Hepes/KCl buffer, in Tris-borate the bI5core RNA is both less compact in the absence of Mg^{2+} and undergoes either an alternate or new conformational change at sub-millimolar Mg^{2+} concentrations (Figure 3C).

bI5core RNA structural neighbors in Hepes/KCl and Tris-borate buffers

We evaluated whether the structure of the bI5core RNA is globally or locally compromised in the Tris-borate buffer using site-specific photocrosslinking. The bI5core RNA was selectively derivatized at the ribose 2′-position at nucleotide U84 (Figure 2B) with a 3-hydroxyphenyl azide group (Figure 2A) (11). Upon photoactivation, the arylazide undergoes ring expansion to form a ketenimine or ketenimine-derived reactant (21). The lifetime of the reactive species is ~100 μs (Figure 2B) and significantly shorter than known RNA folding events (21). The short-lived photoactivated intermediate will thus either form a covalent adduct with a proximal structural neighbor in the RNA or decay by reaction with nucleophilic components of the buffer.

UV radiation of the bI5core RNA, carrying the photocrosslinker at position 84, produces five distinct cross-links (indicated with letters A–E in Figure 4A). These cross-linked species have been previously shown to reflect unimolecular, arylazide-dependent events (21). These cross-links were mapped as stops onto primer extension (11) and are shown superimposed on the bI5core secondary structure in Figure 2A.

Cross-links A, B and C lie close to position 84 in context of the correct bI5core RNA tertiary structure and report structural neighbors that occur selectively in the collapsed and native states (11). In Hepes/KCl, cross-links A, B and C have transition midpoints of 1.2, 1.1 and 1.1, respectively (open circles in Figure 4C). Cross-link D reports the structure of an alternate folding of the P7.1 helix [Figure 2A and (11)]. This cross-link is not significantly populated at low-$MgCl_2$ concentrations, increases in intensity through ~1 mM, and then decreases upon folding to the native state (at 20–40 mM $MgCl_2$) (Figure 4A). The fifth cross-link, E, reflects a structural neighbor that occurs only under Mg^{2+} conditions that favor the expanded state and disappears with a $Mg_{1/2}$ of 1.2 mM (see open circles in cross-link E panel in Figure 4C). These experiments emphasize that significant near-native structure forms in the bI5core RNA with $Mg_{1/2}$s of ~1 mM (Figure 4A). Formation of native structures reported by cross-links A, B and C reflect these individual local interactions. The folding transition monitored by native gel electrophoresis has a slightly higher $Mg_{1/2}$ and reports a global, averaged, collapse of the RNA. Other interactions that contribute to global collapse do form with $Mg_{1/2}$s of ~3 mM [see figure 5D in (11)].

When the photocrosslinking experiments were repeated in Tris-borate, the Mg^{2+}-dependent behavior of the three cross-links, A, B and C, that report native interactions, is essentially indistinguishable from that in Hepes/KCl (Figure 4B; compare open circles and closed squares in Figure 4C). The RNA thus appears folded to the same intermediate collapsed and final native state structures under both buffer conditions. Similarly, the transient cross-link, D, is essentially identical in these buffers.

In strong contrast, the behavior of cross-link E differs in the two buffer systems. Cross-link E reports a non-native interaction between helices P3 and P6 (Figure 2A). With increasing $MgCl_2$ concentrations, this non-native interaction is replaced by the native interaction reported by cross-link C [Figure 2A; see figure 7D in (11)]. In Hepes/KCl, cross-link E decreases monotonically suggesting that the interaction becomes gradually disfavored with increasing $MgCl_2$ concentrations (Figure 4A). In contrast, in Tris-borate, cross-link E is almost undetectable in the absence of magnesium ion, but then grows in intensity until, at ~1 mM Mg^{2+}, it has the same intensity as in the Hepes/KCl buffer system (Figure 4B; see closed squares in the cross-link E panel of Figure 4C). The intermediate reported by cross-link E then decreases in intensity in parallel under both buffer systems (Figure 4).

Thus, in Tris-borate, the structural neighbor reported by cross-link E is selectively destabilized, but not in a way that eliminates formation of this non-native intermediate at higher Mg^{2+} concentrations. Instead, this interaction becomes populated to the same extent as in the Hepes/KCl buffer system (1.6 and 1.9% of total cross-link intensity, respectively) at 1.0 mM $MgCl_2$ (see cross-link E panel in Figure 4C). With increasing Mg^{2+}, loss of the structure reported by cross-link E is indistinguishable in both buffer systems. Therefore, the structure of bI5core RNA is altered in a local way, as judged by photocrosslinking, with folding in other parts of the structure being relatively insensitive to the destabilizing effect of Tris-borate.

An even-more-expanded state in Tris-borate

Extensive prior work has shown that equilibrium folding of the catalytic core of the bI5 group I intron proceeds via formation of a collapsed state prior to reaching the fully folded native state. As judged by site-directed cross-linking, the global structure of the collapsed state RNA is essentially indistinguishable from that in the native state (11). The collapsed state is sufficiently relaxed such that the entire RNA backbone is accessible for cleavage by solvent-based hydroxyl radical chemistry (9) (see collapsed state illustration in Figure 5). The RNA exists in a non-native expanded state at low Mg^{2+} conditions,

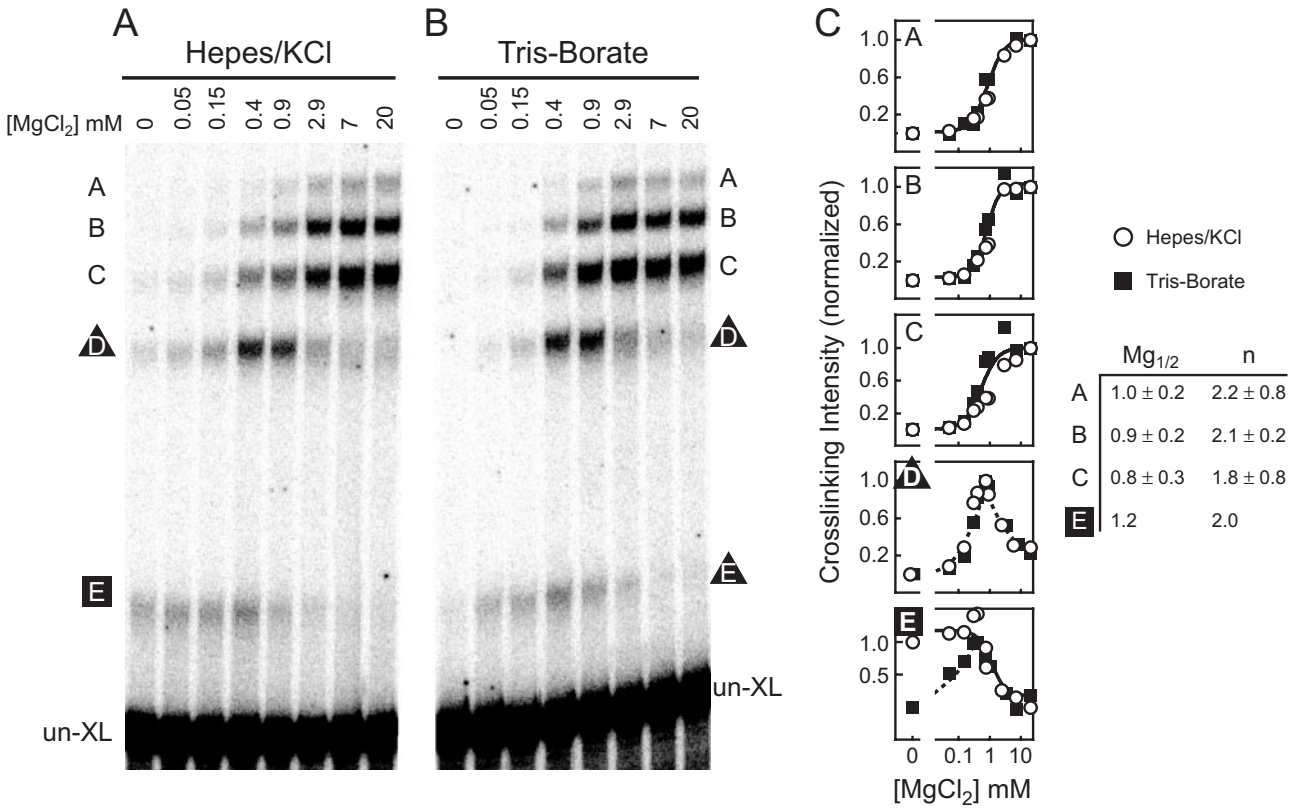

Figure 4. bI5core RNA structures in the vicinity of position 84. Buffer systems are (**A**) Hepes/KCl and (**B**) Tris-borate. Cross-links (A–E) are identified by letters. Triangles indicate transient cross-linking products and the square denotes a non-native interaction populated preferentially at low Mg^{2+} concentrations. (**C**) Quantitative cross-linking profiles in Hepes/KCl (open circles) and Tris-borate (closed squares). For cross-links favored under native state Mg^{2+} conditions (black letters), the average cross-link data from both buffers were fit to normalized cross-linking intensity = $[Mg^{2+}]^n/((Mg_{1/2})^n+[Mg^{2+}]^n)$; where n is the Hill coefficient. Cross-link E, in Hepes/KCl (black box), was fit to 1 minus the above equation. Dashed lines denote qualitative Mg^{2+}-dependent trends in the transient cross-linking data. For clarity, overlapping points are manually offset slightly in the cross-link D and E panels.

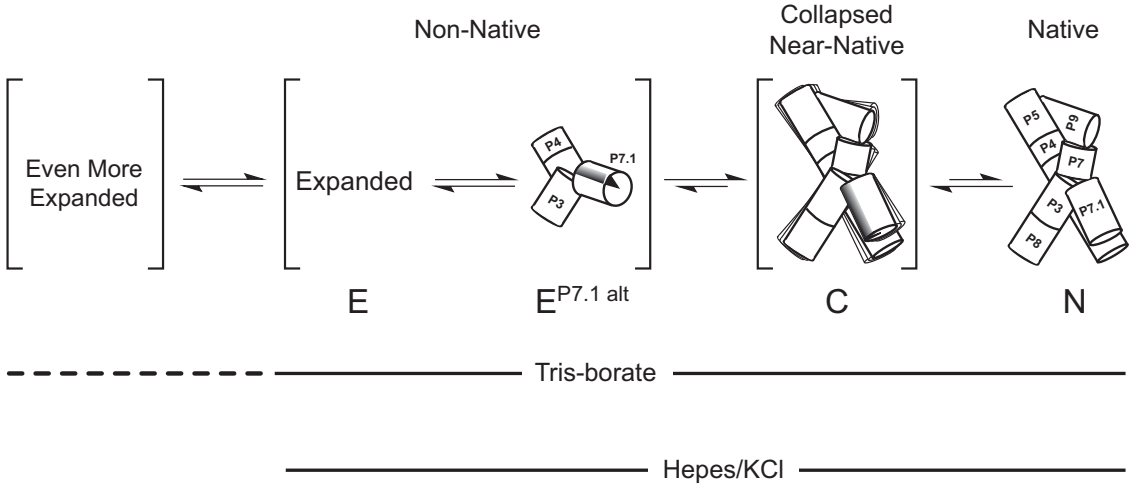

Figure 5. bI5core RNA folding intermediates populated in Hepes/KCl and Tris-borate. Dashed line indicates the non-compact state observed only in Tris-borate at low $MgCl_2$ concentrations.

the near-native collapsed state predominates at intermediate Mg^{2+} concentrations (~7 mM Mg^{2+}), and the native state forms stably at 20–40 mM $MgCl_2$ (19,23) (Figure 5).

The site-directed cross-linking data (Figure 4) demonstrate that the Mg^{2+}-induced folding pathway observed in Tris-borate is identical to that observed in Hepes/KCl once the $MgCl_2$ concentration reaches ~1 mM (emphasized with parallel thin lines for Tris-borate and Hepes/KCl buffers in Figure 5). In the absence of Mg^{2+}, however, native gel electrophoresis experiments show that global collapse of the bI5core

RNA in Tris-borate involves a new, very large amplitude, transition with an apparent $Mg_{1/2}$ of 0.1 mM (Figure 3B and C). Independent evidence for this additional folding transition in Tris-borate is obtained from the buffer-dependent cross-linking profile of cross-link E (compare open circles and closed squares in the cross-link E panel in Figure 4C). The amplitude of the even-more-expanded state to expanded state transition ($Mg_{1/2}$ = 0.14 mM) is so large as to obscure the apparently smaller transition from expanded to collapsed state ($Mg_{1/2}$ = 3.6 mM). The even-more-expanded state, selectively detected at low Mg^{2+} concentrations in Tris-borate, is emphasized by the dashed line in Figure 5.

Destabilization of RNA folding by Tris-borate

Two general classes of mechanism are consistent with the observation that Tris-borate is less able to stabilize RNA folding than Hepes/KCl. First, Tris-borate forms a bulky pseudo-six-membered ring (Figure 1) (12) that may be less able to neutralize charges on the RNA backbone or bind at specific ion sites than the more compact potassium ion. Second, borate anions form stable adducts with carbohydrate hydroxyl groups (17) and also form complexes with nucleic acids, likely via base amino or phosphate oxygen groups (18). Direct adduct formation with borate would compete with the formation of native RNA base pairing and tertiary interactions. Independent of the mechanism, the experimental observation is that use of Tris-borate has an unanticipated effect on RNA structure and folding at low Mg^{2+} concentrations (Figures 3 and 4B) and that Tris-borate by itself is a poor counterion for RNA. In the case of the bI5core RNA, the poor ability of Tris-borate to stabilize RNA folding means that Mg^{2+}-dependent folding must overcome a new structural barrier (Figure 5). Use of Tris-borate should be carefully evaluated prior to using this buffer as a standard state for RNA folding studies.

ACKNOWLEDGEMENT

This work was supported by a grant from the NIH (GM56222) to K.M.W.

REFERENCES

1. Bassi,G.S., Murchie,A.I.H. and Lilley,D.M.J. (1996) The ion-induced folding of the hammerhead ribozyme: core sequence changes that perturb folding into the active conformation. *RNA*, **2**, 756–768.
2. Murchie,A.I., Thomson,J.B., Walter,F. and Lilley,D.M. (1998) Folding of the hairpin ribozyme in its natural conformation achieves close physical proximity of the loops. *Mol. Cell*, **1**, 873–881.
3. Wilson,T.J. and Lilley,D.M.J. (2002) Metal ion binding and the folding of the hairpin ribozyme. *RNA*, **8**, 587–600.
4. Maglott,E.J., Deo,S.S., Przykorska,A. and Glick,G.D. (1998) Conformational transitions of an unmodified tRNA: implications for RNA folding. *Biochemistry*, **37**, 16349–16359.
5. Szewczak,A.A. and Cech,T.R. (1997) An RNA internal loop acts as a hinge to facilitate ribozyme folding and catalysis. *RNA*, **3**, 838–849.
6. Juneau,K. and Cech,T.R. (1999) *In vitro* selection of RNAs with increased structural stability. *RNA*, **5**, 1119–1129.
7. Silverman,S.K., Zheng,M., Wu,M., Tinoco,I.J. and Cech,T.R. (1999) Quantifying the energetic interplay of RNA tertiary and secondary structure interactions. *RNA*, **5**, 1665–1674.
8. Silverman,S.K., Deras,M.L., Woodson,S.A., Scaringe,S.A. and Cech,T.R. (2000) Multiple folding pathways for the P4–P6 RNA domain. *Biochemistry*, **39**, 12465–12475.
9. Buchmueller,K.L., Webb,A.E., Richardson,D.A. and Weeks,K.M. (2000) A collapsed, non-native RNA folding state. *Nature Struct. Biol.*, **7**, 362–366.
10. Bassi,G.S., Murchie,A.I.H., Walter,F., Clegg,R.M. and Lilley,D.M.J. (1997) Ion-induced folding of the hammerhead ribozyme: a fluorescence resonance energy transfer study. *EMBO J.*, **16**, 7481–7489.
11. Buchmueller,K.L. and Weeks,K.M. (2003) Near native structure in an RNA collapsed state. *Biochemistry*, **42**, 13869–13878.
12. Taylor,M.J., Grigg,J.A. and Laban,I.H. (1996) Triol borates and aminoalcohol derivatives of boric acid: their formation and hydrolysis. *Polyhedron*, **15**, 3261–3270.
13. van Duin,M., Peters,J.A., Kieboom,A.P.G. and van Bekkum,H. (1984) Studies on borate esters I. *Tetrahydron*, **40**, 2901–2911.
14. Wenner,J.R. and Bloomfield,V.A. (1999) Buffer effects on EcoRV kinetics as measured by fluorescent staining and digital imaging of plasmid cleavage. *Anal. Biochem.*, **268**, 201–212.
15. Clark,S.M. and Mathies,R.A. (1997) Multiplex dsDNA fragment sizing using dimeric intercalation dyes and capillary array electrophoresis: ionic effects on the stability and electrophoretic mobility of DNA–dye complexes. *Anal. Chem.*, **69**, 1355–1363.
16. Pontius,B.W. and Berg,P. (1991) Rapid renaturation of complementary DNA strands mediated by cationic detergents: a role for high-probability binding domains in enhancing the kinetics of molecular assembly processes. *Proc. Natl Acad. Sci. USA*, **88**, 8237–8241.
17. James,T.D., Sandanayake,K.R.A.S. and Shinkai,S. (1996) Saccharide sensing with molecular receptors based on boronic acid. *Angew. Chem. Int. Ed. Engl.*, **35**, 1910–1922.
18. Stellwagen,N.C., Gelfi,C. and Righetti,P.G. (2000) DNA and buffers: the hidden danger of complex formation. *Biopolymers*, **54**, 137–142.
19. Webb,A.E. and Weeks,K.M. (2001) A collapsed state functions to self-chaperone RNA folding into a native ribonucleoprotein complex. *Nature Struct. Biol.*, **8**, 135–140.
20. Garcia,I. and Weeks,K.M. (2004) Structural basis for the self-chaperoning function of an RNA collapsed state. *Biochemistry*, **43**, 15179–15186.
21. Buchmueller,K.L., Hill,B.T., Platz,M.S. and Weeks,K.M. (2003) RNA-tethered phenylazide photocrosslinking via a short-lived indiscriminant electrophile. *J. Am. Chem. Soc.*, **125**, 10850–10861.
22. Chamberlin,S.I. and Weeks,K.M. (2003) Differential helix stabilities and sites pre-organized for tertiary interactions revealed by monitoring local nucleotide flexibility in the bI5 group I intron RNA. *Biochemistry*, **42**, 901–909.
23. Weeks,K.M. and Cech,T.R. (1995) Protein facilitation of group I intron splicing by assembly of the catalytic core and the 5′ splice site domain. *Cell*, **82**, 221–230.